OSCA: a tool for omic-data-based complex trait analysis

Futao Zhang[1], Wenhan Chen[1], Zhihong Zhu[1], Qian Zhang[1], Ian J. Deary[2], Naomi R. Wray[1,3], Peter M. Visscher[1,3], Allan F. McRae[1], Jian Yang[1,3,4,*]

1. Institute for Molecular Bioscience, The University of Queensland, Brisbane, Queensland 4072, Australia
2. Centre for Cognitive Ageing and Cognitive Epidemiology, Department of Psychology, University of Edinburgh, 7 George Square, Edinburgh, EH8 9JZ, UK
3. Queensland Brain Institute, The University of Queensland, Brisbane, Queensland 4072, Australia
4. Institute for Advanced Research, Wenzhou Medical University, Wenzhou, Zhejiang 325027, China

* Correspondence: Jian Yang (jian.yang@uq.edu.au)

Abstract

The rapid increase of omic data in the past decades has greatly facilitated the investigation of associations between omic profiles such as DNA methylation (DNAm) and complex traits in large cohorts. Here, we proposed a mixed-linear-model-based method (called MOMENT) that tests for association between a DNAm probe and trait with all other distal probes fitted in multiple random-effect components to account for the effects of unobserved confounders as well as the correlations between distal probes induced by the confounders. We demonstrated by simulations that MOMENT showed a lower false positive rate and more robustness than existing methods. MOMENT has been implemented in a versatile software package (called OSCA) together with a number of other implementations for omic-data-based analysis including the estimation of variance in a trait captured by all measures of multiple omic profiles, omic-data-based quantitative trait locus (xQTL) analysis, and meta-analysis of xQTL data.

Introduction

The rapid proliferation of genetic and omic data in large cohort-based samples in the past decade have greatly advanced our understanding of the genetic architecture of omic profiles and the molecular mechanisms underpinning the genetic variation of human complex traits [1-3]. These advances include the identification of a large number of genetic variants associated with gene expression [4, 5], DNA methylation [6, 7], histone modification [8, 9], and protein abundance [10, 11]; the discovery of omic measures associated with complex traits [12, 13]; the improved accuracy in predicting a trait using omic data [14, 15]; and the prioritization of gene targets for complex traits by integrating genetic and omic data in large samples [3, 13, 16-18]. These advances have also led to the development of software tools, focusing on a range of different aspects of omic data analysis. Therefore, a software tool that implements reliable and robust statistical methods for comprehensive analysis of omic data with high-performance computing efficiency is required.

A well-recognised challenge in omic-data-based analysis is to control for false positive rate (FPR) in the presence of confounding factors, as failing to model the confounders may lead to spurious associations [19-21] and/or a loss of statistical power [22]. While some confounders (e.g., age and sex) are known and available in most data so that their effects can be accounted for by fitting them as covariates in linear models, others are either uncharacterised or difficult to measure. For example, in DNA methylation (DNAm) data from whole blood, cell type compositions (CTCs) are evident confounders in a methylome-wide association study (MWAS; also known as an epigenome-wide association study or EWAS) [21, 23, 24] although CTCs may be useful for the prediction of some phenotypes. CTCs tend to be correlated with the DNAm at CpG sites that are differentially methylated in different cell types (namely differentially methylated sites) and have been shown to be associated with age and multiple traits and diseases [19, 21, 25, 26]. MWAS analysis without accounting for CTCs could give rise to biased test-statistics unless neither CTCs nor DNAm sites are associated with the trait in question. Although it is possible to measure CTCs directly or predict them by reference-based prediction methods [27, 28], reference-free methods that are able to correct for confounding effects without the need of characterizing all the confounders have broader applications [22, 29-32]. Moreover, the predicted CTCs often only explain a certain proportion of variation in CTCs resulting in biased test-statistics due to the uncaptured variation in CTCs. Existing reference-free methods are mainly based on the strategy of fitting a number of covariates (estimated from factor analysis or similar approaches with or without reference [22, 29, 31, 32]) in a fixed-effect model or a set of selected DNAm probes in a mixed linear model (MLM) [30]. However,

uncharacterized confounders with small to moderate effects and numerous correlations between distal DNAm probes (e.g. those on different chromosomes) induced by the confounders may not be well captured by either a fixed number of principal features or a subset of selected probes.

In this study, we proposed a reference-free method (called MOA: MLM-based omic association) that fits all probes as random effects in an MLM-based association analysis to account for the confounding effects, including the correlations among distal probes induced by the confounding. We then extended the method to stratify the probes into multiple random-effect components (called MOMENT: multi-component MLM-based omic association excluding the target) to model a scenario where some probes are much more strongly associated with the phenotype than others. We evaluated the performance of MOA and MOMENT by extensive simulations and demonstrated their reliability and robustness in comparison with existing methods. We have implemented MOA and MOMENT together with a comprehensive set of other methods for omic data analysis in an easy-to-use and computationally efficient software package, OSCA (omic-data-based complex trait analysis).

Results

Overview of the OSCA software

OSCA comprises four main modules: 1) data management for which we designed a binary format to efficiently store and manage omic data; 2) linear-regression- and MLM-based methods (including the methods proposed in this study) to test for associations between omic measures and complex traits; 3) methods to estimate the proportion of variance in a complex trait captured by all the measures of one or multiple omic profiles (e.g., all SNPs and DNAm probes), and to predict the trait phenotype in a new sample based on the joint effects of all omic measures estimated in a discovery sample; and 4) an efficient implementation of the methods to identify genetic variants associated with an omic profile, e.g., DNA methylation quantitative trait loci (mQTL) analysis. We will describe the methods based on DNAm data but the methods and software tool are in principle applicable to other types of omic data including gene expression, DNAm, histone modification, and protein abundance. The computer code of OSCA is written in C++ programming language and supports multi-threading based on OpenMP for high-performance computing. The compiled binary files are freely available at http://cnsgenomics.com/software/osca/.

MLM-based omic association analysis methods

One of the primary applications of OSCA is to test for associations between omic measures (e.g. DNAm probes) and a complex trait (e.g. body mass index (BMI)) correcting for confounding effects. In an MWAS, the test-statistics of null probes can be inflated because of the associations of probes with confounders that are correlated with the phenotype. Note that, even if the confounders are not directly associated with the phenotype, the presence of confounders (e.g., CTCs or experimental batches) can cause correlations between the trait-associated probes and the null probes in distal genomic regions or even on different chromosomes, giving rise to inflated test-statistics of the null probes (see the simulation results below). Existing methods that fit a number of covariates computed from dimension reduction approaches in a fixed-effect model [22, 31, 32] or a set of selected DNAm probes in an MLM [30] may not be sufficient to correct for confounding effects widely spread among a large number of probes or correlations between distal probes induced by the confounding. We propose two MLM-based approaches (MOA and MOMENT) that include all the (distal) probes as random effects in the model to account for the effects of the confounders on the trait and probes as well as the correlations among distal probes. We show by simulations (see below) that both MOA and MOMENT are more robust than existing methods in controlling for false positive rate (FPR) and family-wise error rate (FWER) in MWAS (see below).

Here we start with a general model that fits all probes as random effects, i.e.,

$$\mathbf{y} = \mathbf{C}\boldsymbol{\beta} + \mathbf{W}\mathbf{u} + \mathbf{e} \qquad [1]$$

where $\mathbf{y}$ is an $n \times 1$ vector of phenotype values with n being the sample size, $\mathbf{C}$ is an $n \times p$ matrix for covariates (e.g., age and sex) with p being the number of covariates, $\boldsymbol{\beta}$ is a $p \times 1$ vector of the effects of covariates on the phenotype, $\mathbf{W}$ is an $n \times m$ matrix of standardised DNAm measures of all m probes, $\mathbf{u}$ is an $m \times 1$ vector of the joint effects of all probes on the phenotype, and $\mathbf{e}$ is an $n \times 1$ vector of residuals. In this model, $\boldsymbol{\beta}$ are fixed effects whereas $\mathbf{u}$ and $\mathbf{e}$ are random effects with $\mathbf{u} \sim N(\mathbf{0}, \mathbf{I}\sigma_u^2)$ and $\mathbf{e} \sim N(\mathbf{0}, \mathbf{I}\sigma_e^2)$. The variance-covariance matrix for $\mathbf{y}$ is $\mathrm{var}(\mathbf{y}) = \mathbf{V} = \mathbf{W}\mathbf{W}'\sigma_u^2 + \mathbf{I}\sigma_e^2$. This equation can be re-written as

$$\mathbf{V} = \mathbf{A}\sigma_o^2 + \mathbf{I}\sigma_e^2 \text{ with } \mathbf{A} = \mathbf{W}\mathbf{W}'/m \text{ and } \sigma_o^2 = m\sigma_u^2 \qquad [2]$$

where $\mathbf{A}$ is defined as the omic-data-based relationship matrix (ORM) (**Methods**) and σ_o^2 is the amount of phenotypic variance captured by all probes. The variance components (σ_o^2 and σ_e^2) in such an MLM can be estimated by REML algorithms [33]. Analogous to the method for estimating SNP-based heritability [34, 35], the proportion of variance in the phenotype captured by all the probes can be defined as $\rho^2 = \sigma_o^2/(\sigma_o^2 + \sigma_e^2)$. We name this variance-estimation method OREML following the nomenclature of GREML [34]. The estimated joint probe effects ($\hat{\mathbf{u}}$) from this model by

a random-effect estimation approach (e.g. BLUP [36]) can be used to predict the phenotypes of individuals in a new sample based on omic data, i.e., $\hat{\mathbf{y}}_{\text{new}} = \mathbf{W}_{\text{new}}\hat{\mathbf{u}}$. We call this OBLUP analysis.

Model [1] can be extended to test for association between a probe *i* and the trait, i.e.,

$$\mathbf{y} = \mathbf{w}_i b_i + \mathbf{C}\boldsymbol{\beta} + \mathbf{W}\mathbf{u} + \mathbf{e} \text{ with } \mathbf{V} = \mathbf{W}\mathbf{W}'\sigma_u^2 + \mathbf{I}\sigma_e^2 \qquad [3]$$

In comparison to model [1], model [3] has two additional terms, $\mathbf{w}_i$ (an $n \times 1$ vector of standardised DNAm measures of a probe *i*, i.e., the target probe) and b_i (the effect of probe *i* on the phenotype; fixed effect). The probe effect b_i (together with the covariates' effects) can be estimated by the generalized least squares (GLS) approach, i.e., $\left[\hat{b}_i\ \hat{\boldsymbol{\beta}}\right]' = (\mathbf{X}'\mathbf{V}^{-1}\mathbf{X})^{-1}\mathbf{X}'\mathbf{V}^{-1}\mathbf{y}$ and $\text{var}\left[\hat{b}_i\ \hat{\boldsymbol{\beta}}\right]^T = (\mathbf{X}'\mathbf{V}^{-1}\mathbf{X})^{-1}$ with $\mathbf{X} = [\mathbf{w}_i\ \mathbf{C}]$. The sampling variance (standard error (SE) squared) of $\hat{b}_i$ is the first diagonal element of $\text{var}\left[\hat{b}_i\ \hat{\boldsymbol{\beta}}\right]^T$. The null hypothesis ($H_0$: $b_i = 0$) can be tested by a two-sided *t*-test (or approximately chi-squared test if sample size is large) given $\hat{b}_i$ and its SE. We call this method MOA. Applying this method to test each of the probes across the genome is extremely computationally expensive because the variance components σ_u^2 and σ_e^2 need to be estimated repeatedly for each probe by REML that requires the computation of $\mathbf{V}^{-1}$ (computational complexity of $O(n^3)$) multiple times in an iterative process. To speed up the computation, we use a two-step approach as in [37] to compute $\mathbf{V}^{-1}$, with the first step to perform an eigendecomposition of $\mathbf{W}\mathbf{W}'$ and the second step to compute $\mathbf{V}^{-1}$ based on the eigenvalues and eigenvectors. Since the eigendecomposition only needs to be done once for the whole genome scan, this two-step approach reduces the complexity of computing $\mathbf{V}^{-1}$ by orders of magnitude when testing each specific probe. Moreover, as the proportion of phenotypic variance attributable to a single probe is often very small, we can further speed up the computation by an approximate approach (similar to the approximate MLM-based GWAS methods [38, 39]) that only requires to compute $\mathbf{V}^{-1}$ once, assuming that the estimates of σ_u^2 and σ_e^2 under the null (i.e., $b_i = 0$) are approximately equal to those under the alternative (i.e., $b_i \neq 0$). Both the approximate and exact MOA approaches have been implemented in OSCA.

There are two properties of the MOA method worthy of consideration. First, the target probe is fitted twice in the MOA model, once as a fixed effect (b_i) and again as a random effect (the *i*-th element of $\mathbf{u}$), resulting in a loss of power to detect b_i (a recognised issue in MLM-based association analysis with SNP data [39, 40]). This problem can be solved by leaving out probes in close physical proximity of the target probe (including the target) from the random-effect term because DNAm status of CpG sites in close physical proximity are likely to be regulated by the same mechanism and

157 therefore tend to be highly correlated. This strategy has been used previously in both GWAS
158 (genome-wide association study) [39, 40] and MWAS [30]. In practice, we exclude the probes <50Kb
159 from the target probe (note that the distance parameter may differ for other types of omic data).
160 Second, MOA assumes a single distribution to all the probe effects in the random-effect term, which
161 may not be well fitted to data if some probes have much stronger associations with the trait than
162 other probes. For example, if CTCs are associated with the phenotype, then all the probes that are
163 highly differentially methylated in different cell types [41-43] may present a very different
164 distribution of effects from the other probes. One solution to this issue is to stratify the probes into
165 multiple groups by the association test statistics (from linear regression) and fit them as separate
166 random-effect terms in the model. We extended the MOA method with the two modifications
167 mentioned above and named it as MOMENT (multi-component MLM-based omic association
168 excluding the target). The MOMENT model can be written as

169 $$\mathbf{y} = \mathbf{w}_i b_i + \mathbf{C}\boldsymbol{\beta} + \sum_j \mathbf{W}_j \mathbf{u}_j + \mathbf{e} \text{ with } \mathbf{V} = \sum_j \mathbf{W}_j \mathbf{W}_j{}' \sigma_{u_j}^2 + \mathbf{I}\sigma_e^2 \qquad [4]$$

170 where $\mathbf{W}_j$ is an $n \times m_j$ matrix of standardised DNAm measures of the probes in the j-th group with
171 m_j being the number of probes in the group (excluding the probes <50Kb from the target probe). In
172 practice, the probes are split into two groups by association p-values from a linear regression model
173 (i.e., $\mathbf{y} = \mathbf{w}_i b_i + \mathbf{C}\boldsymbol{\beta} + \mathbf{e}$) at a genome-wide significant threshold (or by the proportion of phenotypic
174 variance captured per probe at a certain threshold). The GLS method described in model [3] can be
175 used to estimate b_i and its SE for hypothesis testing with $\sigma_{u_j}^2$ and σ_e^2 (under the null) re-estimated
176 every time when a different set of probes are excluded from the random-effect terms.
177

178 **Simulation analysis**

179 To quantify the false positive rate (or family-wise error rate) and statistical power of MOMENT
180 (implemented in OSCA), we performed simulations based on DNAm and CTCs [44] measures on
181 samples from the Lothian Birth Cohorts (LBC) in three scenarios (**Supplementary Note 1**). That is,
182 we simulated a phenotype: 1) with effects from a set of "causal probes" (randomly selected from all
183 probes on the odd chromosomes) but no direct effects from the CTCs; 2) with small to large effects
184 from CTCs but no effects from the probes; and 3) with effects from both the causal probes and CTCs
185 (**Supplementary Note 1**). Note that we only sampled the causal probes from the odd chromosomes
186 in scenarios 1 and 3, leaving the probes on the even chromosomes to quantify false positive rate
187 under the null, and that the DNAm measures were adjusted for age, sex, experimental batches, and
188 smoking status. Results from our models were compared to 6 different methods including: 1) Unadj:
189 linear regression without adjustment; 2) CTCadj: linear regression with CTCs fitted as covariates. 3)

190 SVA: linear regression with the SVA surrogate variables fitted as covariates [22]; 4) LFMM2-ridge: a
191 latent factor mixed model (LFMM) using ridge algorithm for confounder estimation [32]; 5) LFMM2-
192 lasso: an LFMM using lasso algorithm for confounder estimation [32]; 6) ReFACTor: linear
193 regression with the first 5 sparse principal components (PCs) from ReFACTor fitted as covariates
194 [31]; 7) 5PCs: linear regression with the first 5 PCs, computed from a principal component analysis
195 (PCA), fitted as covariates; and 8) FaST-LMM-EWASher: a set of selected probes fitted as random
196 effect in an MLM [30]. For completeness of the analysis, we also included MOA (implemented in
197 OSCA) in the comparison. We validated using a subset of data generated from simulation scenario 1
198 that the approximate MOA approach was almost identical to the exact approach (**Supplementary**
199 **Figure 1**). Hence, for the ease of computation, we used the approximate MOA approach in all the
200 subsequent analyses.
201
202 In simulation scenario 1, although there were no direct effects of the CTCs on the phenotype, the
203 test-statistics from Unadj at the null probes were inflated (**Figure 1a** and **Supplementary Table 1**)
204 because the null and causal probes, although on different sets of chromosomes, are correlated
205 through their correlations with systematic biases such as CTCs. The mean genomic inflation factor
206 (λ) [45] of the null probes (on the even chromosomes) from 100 simulation replicates was 7.67 for
207 Unadj (**Supplementary Table 1**), where λ is defined as the median of χ^2 test-statistics of the null
208 probes divided by its expected value. CTCadj reduced but not completely removed the inflation in
209 test-statistics of the null probes (**Figure 1a** and **Supplementary Table 1**), suggesting that the
210 inflation was caused by correlations between the causal and null probes because of the confounding
211 effects of both CTCs and other unobserved confounders. While all the other methods were much less
212 inflated compared to Unadj, MOMENT and MOA showed the least inflation with a mean λ value close
213 to 1. It is slightly surprising to observe that the family-wise error rates (FWERs) of all the methods
214 except MOA and MOMENT were highly inflated (FWERs > 0.6) (**Supplementary Figure 2a** and
215 **Supplementary Table 1**) despite the relatively small genomic inflation at the null probes for most
216 of the methods (**Figure 1a**). Here, FWER is defined as the proportion of simulation replicates with
217 at least one null probe at MWAS p-value < 0.05 / m with m being the number of null probes, which
218 can be interpreted as the probability of observing one or more false positives at a genome-wide
219 significance level in a single experiment. There was no inflation in FWER for MOMENT, and a
220 marginal inflation for MOA (**Supplementary Figure 2a** and **Supplementary Table 1**), showing the
221 effectiveness of using all (distal) probes to account for the probe correlations. We also quantified
222 the FPR, defined as the proportion of null probes with p-values < 0.05 in each simulation replicate.

The differences in FPR among the methods showed a similar pattern to the differences in genomic inflation factor (**Supplementary Figure 2b** and **Supplementary Table 1**). We then compared power among the methods. Since the test-statistics of many approaches were highly inflated, it is not very meaningful to compare power without accounting for the inflation. We therefore used the Area Under the ROC Curve (AUC) to compare power of the methods given the same level of FPR. Apart from Unadj and CTC, the AUCs of all the methods were on similar levels (**Figure 1b**). The conclusions held in additional simulations varying the number of causal probes and the proportion of phenotypic variance captured by the causal probes (**Supplementary Figures 3** and **4**) despite that the inflation in FWER for the existing methods appeared to increase with the increase of the proportion of variance captured per causal probe. Additionally, we applied BACON, a summary-data based method that seeks to remove genomic inflation taking the true positives into consideration, to the test-statistics of all probes produced by the methods tested above. We showed that the inflation in test-statistics of the null probes for Unadj was substantially reduced but not completely removed by the BACON adjustment and that the test-statistics from MOA and MOMENT remained almost unchanged after the BACON adjustment (**Supplementary Figure 5**).

In simulation scenario 2 where there is no direct probe-trait association, all the probes are null and their χ^2 test-statistics are expected to follow a χ^2 distribution with 1 degree of freedom if the effects of CTCs have been well accounted for. The results showed that the λ value was close to 1 for all the methods except Unadj and FaST-LMM-EWASher (**Figure 2a**). It seems that, for some of the methods (e.g. 5PCs and ReFACTor), the λ value slightly increased with the increase of the proportion of variance explained by the CTCs (R^2_{CTCs}) (**Figure 2a**). The FPRs of the methods were highly consistent with the genomic inflation factors (**Supplementary Figure 6**). Nevertheless, a non-inflated median test-statistic does not necessarily mean that the FWER has been well controlled for. In fact, most methods showed inflated FWER in this simulation scenario, and the FWERs of all the methods increased with increasing R^2_{CTCs} (**Figure 2b**). The FWERs of 5PCs, ReFACTor, LFMM2-ridge, and LFMM2-lasso were close to the expected value (i.e., 0.05) when $R^2_{\mathrm{CTCs}} = 0.005$ and increased to a level between 0.15 and 0.2 when $R^2_{\mathrm{CTCs}} = 0.05$ (**Figure 2b**). The relationship between FWER and R^2_{CTCs} was relatively flat for SVA with its FWER varying from 0.05 to 0.1 when R^2_{CTCs} increased from 0.005 to 0.05. Although FaST-LMM-EWASher showed the most deflated test-statistics among all the methods (**Figure 2a**), its FWER was substantially higher than all the other methods except Unadj (**Figure 2b**), likely due to its feature selection strategy (**Supplementary Note 2**). MOA and MOMENT performed similarly in this simulation scenario and showed the lowest

256 inflation in FWER among all the methods with their FWER being lower than 0.05 when R^2_{CTCs} =
257 0.005 and increased to about 0.1 when R^2_{CTCs} = 0.05 (**Figure 2b**). In addition, we performed a linear
258 regression analysis with the known CTCs fitted as covariates; as expected, the FWER of was close to
259 0.05 irrespective of the level of R^2_{CTCs} (see below for the analysis with predicted CTCs).
260
261 We also compared the methods under the circumstance (simulation scenario 3) where there were
262 associations between the phenotype and CTCs ($R^2_{\mathrm{CTCs}} = 0.05$) and the null probes were correlated
263 with distal causal probes because both of them were correlated with CTCs (**Supplementary Note**
264 **1**). The results were similar to those above (**Figure 1** and **Supplementary Figure 2**). That is, the
265 FWER of MOMENT was close to the expected value, demonstrating the reliability and robustness of
266 the method. The FWER of MOA is slightly higher than that of MOMENT but much lower than those of
267 the other methods that showed strong inflation in FWER and/or FPR due to the correlations
268 between causal and null probes (**Supplementary Figures 7a, 6c** and **6d**, and **Supplementary**
269 **Table 2**). All the methods showed similar levels of AUC except for Unadj and CTCadj
270 (**Supplementary Figure 7b**). The conclusions held with different sample sizes (**Supplementary**
271 **Figures 8** and **9**) or different numbers of causal probes with smaller or larger variance explained
272 per causal probe (**Supplementary Figures 10** and **11**). The conclusions also held if we simulated
273 confounding effects on experimental batches in lieu of CTCs (**Supplementary Figures 12** and **13**).
274 We further demonstrated the consistency of the result from MOA/MOMENT analysis of the whole
275 sample and the result from a meta-analysis of summary statistics from MOA/MOMENT analyses in
276 two halves of the sample (**Supplementary Figure 14**).
277
278 We further compared runtime and memory usage of the methods using data generated in
279 simulation scenario 1 (**Supplementary Table 3**). We found that MOA and MOMENT showed the
280 lowest memory usage among all the methods. The approximate MOA approach was the second
281 fastest approach (only slightly slower than LFMM2-ridge) and MOMENT was slower than LFMM2-
282 ridge, approximate MOA and ReFACTor but much faster than SVA, LFMM2-lasso and EWASher.
283
284 **An application of MOMENT to real data**
285 We applied MOMENT and the other methods to four real quantitative traits in the LBC cohorts.
286 These traits, including BMI, height, lung function (measured in the highest score of forced expiratory
287 volume in one second), and walking speed (measured in the time taken to walk 6 meters), were
288 standardised and corrected for age in each gender group within each sub-cohort (LBC1936 or

LBC1921) (**Methods**). The standardised phenotypes were further processed by a rank-based inverse-normal transformation. The DNAm probes were adjusted for age, sex, and experimental batches. We did not adjust the probes for CTCs or smoking status for the purpose of testing methods (see below).

Consistent with the results from simulations, the test-statistics from MOA and MOMENT were not inflated whereas all the other methods showed modest inflation for all the traits (**Figure 3, Table 1,** and **Supplementary Figures 15-18**). There were three associations that were identified by multiple methods, including one for BMI (cg11202345, detected by all methods), in line with a previous study [46], and two for lung function (cg05575921 and cg05951221, detected by all methods except MOMENT) (**Supplementary Table 4, Supplementary Figures 15** and **17**). It should be noted that cg05575921 was reported to be associated with smoking in a previous study [47], indicating that the association between cg05575921 and lung function might be confounded by smoking status. Moreover, MOA, LFMM2-ridge, LFMM2-lasso, and ReFACTor consistently identified 12 additional probes associated with lung function but most of the probes have been linked to smoking in a previous study [48]. Almost all the associations were not significant when smoking status was fitted as a covariate in the models (6.5% of variance in lung function associated with smoking status; **Supplementary Table 5** and **Supplementary Figure 19**), suggesting that most (if not all) of the probe associations with lung function identified by the four methods mentioned above were owing to the confounding of smoking. None of the smoking-associated probes were genome-wide significant for lung function in the analysis using MOMENT (**Supplementary Figure 17**) and the result remained the same when smoking status was fitted as a covariate in MOMENT (**Supplementary Figure 19**), again demonstrating showing the capability of MOMENT in correcting for unobserved confounding factors.

It has been shown in previous GWASs that MLM-based association analysis methods developed for quantitative traits are applicable to discrete traits including ascertained case-control status [37-39, 49]. To demonstrate the applicability of the proposed methods to discrete phenotypes, we analysed smoking status (non-smoker, former smoker or current smoker; coded as 0, 1 or 2) in the LBC by MOA and MOMENT in comparison with the existing methods. All the methods detected a large number (at least 112) of probes at a genome-wide significance level (P < 2.19e-7) except for MOMENT and EWASher which only identified 4 and 2 genome-wide significant probes, respectively (**Supplementary Figure 20**). To validate the association signals other than those identified by

322 MOMENT, we fitted the 4 MOMENT probes as fixed covariates in MOA. None of the additional
323 associations remained genome-wide significant conditioning on the 4 MOMENT probes
324 (**Supplementary Figure 21**), suggesting that those additional associations detected by MOA (and
325 other methods) were driven by their correlations with the 4 MOMENT signals. MOA failed in this
326 scenario likely because the associations of the 4 MOMENT signals were too strong to be fitted in a
327 signal normal distribution with the other probes. This conclusion is further supported by the result
328 that the accuracy of predicting/classifying smoking status in a cross-validation setting using the
329 large number of probes detected by linear regression or MOA was even lower than that using the
330 small number of probes detected by MOMENT (**Supplementary Table 6**). In addition, we recoded
331 the smoking status data to a binary phenotype (0 for non-smoker and 1 for former or current
332 smoker) and applied all the methods to the recoded binary phenotype; the conclusions were similar
333 as above but it seemed that the analyses with the binary phenotype were less powerful than those
334 with the categorical phenotype above (**Supplementary Figure 22**). All these results show the
335 applicability of MOMENT to discrete traits and again demonstrate the robustness and reliability of
336 MOMENT in controlling for false positive associations.
337
338 **Estimating variance in a phenotype captured by all probes by OREML**
339 We have demonstrated the performance of the omic-data-based association analysis methods in
340 OSCA by simulation and real data analysis. We then turned to evaluate the performance of OREML
341 in estimating the proportion of variance in a complex trait captured by all probes (ρ^2) by simulation
342 in two scenarios (**Supplementary Note 1**). The results showed that under either scenario, OREML
343 reported an unbiased estimate of ρ^2 (**Supplementary Table 7**). Here the unbiasedness is defined as
344 that the mean ρ^2 estimate from 500 independent simulations is not significantly different from the
345 ρ^2 parameter used in the simulation. There are two methods implemented in OSCA to compute the
346 ORM (**Methods**). Our simulation results showed that the estimates of ρ^2 based on the two methods
347 were similar (**Supplementary Table 7**).
348
349 We also attempted to partition and estimate the proportions of phenotypic variation captured by all
350 SNPs (i.e., h^2_{SNP}) and all the DNAm probes respectively when they were fitted jointly in one model.
351 We first investigated the correlation between genomic relationship matrix (GRM) and methylomic
352 relationship matrix (MRM) in the LBC dataset. We found that the off-diagonal elements of the GRM
353 were almost independent of those of the MRM (r = 0.0045; **Supplementary Figure 23**). From an
354 OREML analysis that fits the GRM and MRM jointly, we estimated that all the DNAm probes captured

355 6.5% (SE = 0.038) of the variance for BMI but the estimate for height was nearly zero ($\hat{\rho}^2$ = -0.005
356 and SE = 0.0086) (**Supplementary Table 8**). These results are in line with the finding from a
357 previous study that the accuracy of genetic risk prediction can be improved by incorporating DNAm
358 data for BMI but not height [14].

359 **Discussion**

360 In this study, we developed a versatile software tool—OSCA—to manage omic data generated from
361 high-throughput experiments in large cohorts and to facilitate the analyses of complex traits using
362 omic data (**Supplementary Note 4**). The primary applications of OSCA are to identify omic
363 measures associated with a complex trait accounting for unobserved confounding factors
364 (MOMENT) and to estimate the proportion of phenotypic variation captured by all measures of one
365 or multiple omic profiles (OREML). A by-product of the OREML application is to estimate the joint
366 effects of all measures of one or multiple omic profiles (i.e., OBLUP analysis) to predict the
367 phenotype in a new sample. This has been shown to be a powerful and robust approach in age
368 prediction using gene expression or DNAm data [50, 51]. We have also provided computationally
369 efficient implementations in OSCA to manage large-scale omic data, and to perform omic-data-based
370 quantitative trait locus (xQTL) analysis and meta-analysis of xQTL summary data. OSCA is an
371 ongoing software development project so that any further methods or functions related to omic-
372 data-based analysis can be included in the software package in the future.
373
374 We showed, by simulation, a surprisingly high error rate for all the existing MWAS/EWAS methods,
375 mainly owing to the correlations between distal probes induced by CTCs (and/or other systematic
376 biases) in DNAm data (**Figure 1**). These correlations are widespread at a large number of probes
377 across the genome (as demonstrated by the proportion of null probes with $P_{\mathrm{MWAS}} < 0.05$ in
378 simulation scenario 1; **Supplementary Figure 24**) and thus are not adequately accounted for by a
379 fixed number of principal features computed from the data (e.g. 5PCs, ReFACTor, LFMM2, and SVA)
380 nor a set of selected probes (e.g. FaST-LMM-EWASher). This conclusion is likely to be applicable to
381 other types of omic data if the measures in distal genomic regions are correlated due to unmeasured
382 confounding factors such as systematic experimental biases or unwanted biological variation. We
383 show by simulation that this confounding effect can be corrected for by fitting the target probe as a
384 fixed effect and all the other (distal) probes as random effects (i.e., the MOA or MOMENT method).
385 In addition, we also tested the robustness of MOMENT to the change of window size used to exclude
386 probes in close physical proximity to the target probe in either direction. We varied the window size

387 from 100Kbp to 250bp in the MOMENT analysis of data generated from simulation scenario 1
388 (**Supplementary Figures 25**). We found that the results remained almost unchanged when the
389 window sizes decreased from 100Kbp to 25Kbp whereas there were a substantial number of probes
390 showing deflated test-statistics when the window size decreased to 500bp or 250bp
391 (**Supplementary Figures 25**). These results justify the use of 50Kbp as the default window size for
392 MOMENT in OSCA.
393
394 Our simulation also showed that, if CTCs or batches explain a large proportion of variation in the
395 phenotype, the FWERs of all the methods tended to be inflated (**Supplementary Figures 26** and
396 **27**) despite that the genomic inflation factor is close to unity for most methods (**Figure 2**). We re-
397 ran the simulation under a more extreme setting with R^2_{CTCs} varying from 10% to 70%. In this case,
398 the genomic inflation factors of the fixed-effect models (i.e., SVA, ReFACTor, LFMM2, and 5PCs) and
399 the FWERs of all the methods increased as R^2_{CTCs} increased (to a lesser extent for FaST-LMM-
400 EWASher), suggesting that there were a set of probes strongly associated with CTCs
401 (**Supplementary Figure 28**). Note that even in this extreme case, MOMENT showed the lowest
402 FWERs on average amongst all the methods. It is also of note that the FWERs of FaST-LMM-
403 EWASher was relatively low in this scenario (**Supplementary Figure 26**), opposite to its
404 performance when R^2_{CTCs} was low (**Figure 2**), possibly due to its variable selection strategy
405 (**Supplementary Note 2**). The inflation in FWER was only slightly alleviated by fitting the predicted
406 CTCs as covariates (**Supplementary Figures 29** and **30**). The results also suggest that it may be
407 worth fitting measured CTCs as fixed-effect covariates in MLM-based association analyses such as
408 MOA and MOMENT in practice although this approach is likely to be conservative as indicated by
409 the deflated λ and FWER (**Supplementary Figure 31**). These conclusions are likely to be applicable
410 to other confounding factors such as smoking status, as demonstrated in the real data analysis for
411 lung function (**Supplementary Figure 19**). Our results also caution the interpretation of
412 associations identified from MWAS for traits that are highly correlated with CTCs and/or other
413 biological confounders.
414
415 In conclusion, we showed by simulation the inflation in test-statistics of the existing MWAS methods
416 because of the ubiquitous correlations between distal probes caused by confounding factors, and
417 developed two new MWAS methods (MOA and MOMENT) to correct for the inflation. We
418 demonstrated the reliability and robustness of MOMENT by simulations in a number of scenarios
419 and real data analysis. We recommend the use of MOMENT in practice because of its robustness in

420 the presence of unobserved confounders despite that it is slightly less powerful than MOA. We
421 implemented both MOA and MOMENT in a computationally efficient and easy-to-use software tool
422 OSCA together with many other functions for omic-data-based analyses (**Supplementary Figure**
423 **32**).
424

425 **Methods**

426 **Omic-data-based relationship matrix (ORM)**

427 We have described in equations [1] and [2] the OREML model to estimate the proportion of variance
428 in a phenotype captured by the DNAm probes all together. In equation [1], i.e., $\mathbf{y} = \mathbf{C\beta} + \mathbf{Wu} + \mathbf{e}$, we
429 define $\mathbf{W}$ as a matrix of standardised measures of DNAm probes, and in equation [2] we define the
430 ORM as $\mathbf{A} = \mathbf{WW}'/m$. Therefore, the omic relationship between individual j and k (the jk-th element
431 of $\mathbf{A}$) can be computed as $A_{jk} = \frac{1}{m}\sum_i (x_{ij} - \mu_i)(x_{ik} - \mu_i)/\sigma_i^2$, where x_{ij} is the unstandardised DNAm
432 level of probe i in individual j, μ_i and σ_i^2 are the mean and variance of the i-th probe over all the
433 individuals respectively, and m is the number of probes. This model implicitly assumes that the
434 probes of smaller variance in DNAm level (unstandardised) tend to have larger effects on the
435 phenotype (strictly speaking, stronger associations with the phenotype), and that there is no
436 relationship between the proportion of trait variance captured by a probe and the variance of the
437 probe. We also provide in OSCA an alternative method to compute the ORM, i.e., $A_{jk} = \sum_i (x_{ij} -$
438 $\mu_i)(x_{ik} - \mu_i) / \sum_i \sigma_i^2$. If we use this definition of ORM in the OREML analysis, we implicitly assume
439 that there is no relationship between the probe effect on the trait and the variance of the probe but
440 the proportion of trait variance associated with a probe increases as the variance of the probe
441 increases. We showed by simulation and real data analysis that the difference between the OREML
442 results using the two methods was very small (**Supplementary Tables 7** and **8**).

443

444 **OREML: estimating the proportion of trait variance captured by all DNAm probes**

445 We have shown in equations [1] and [2] an OREML model with one random-effect component to
446 estimate the proportion of trait variance captured by all DNAm probes. The model is flexible and
447 can be extended to partition the trait variance into components associated with different sets of
448 probes (e.g. a model with 22 components with all the probes on each chromosome as a component).
449 A flexible OREML model can be written as

450 $\mathbf{y} = \mathbf{C\beta} + \sum_i \mathbf{W}_i\mathbf{u}_i + \mathbf{e}$ with $\mathrm{var}(\mathbf{y}) = \mathbf{V} = \sum_i \mathbf{W}_i\mathbf{W}_i{}'\sigma_{u_i}^2 + \mathbf{I}\sigma_e^2 = \sum_i \mathbf{A}_i\sigma_{o_i}^2 + \mathbf{I}\sigma_e^2$

451 where the definitions of all the parameters and variables are similar to those in equations [1] and
452 [2].The variance components can be estimated by REML [33], and the proportion of the trait
453 variance captured by the i-th component can be computed as $\rho_i^2 = \sigma_{o_i}^2/(\sum_i \sigma_{o_i}^2 + \sigma_e^2)$.

454

455 The multi-component OREML model can be applied to partition the trait variance into components
456 associated with multiple omic profiles. For example, if SNP genotype, DNAm, and gene expression
457 data are available for all the individuals in a cohort, a multi-component OREML model can be used

458 to estimate the proportion of trait variance captured by all SNPs (i.e., the SNP-based heritability),
459 the expression levels of all genes, and the DNAm levels at all the CpG sites. The model can be written
460 as $\mathbf{y} = \mathbf{C\beta} + \mathbf{W}_g\mathbf{u}_g + \mathbf{W}_t\mathbf{u}_t + \mathbf{W}_m\mathbf{u}_m + \mathbf{e}$ with $\mathrm{var}(\mathbf{y}) = \mathbf{A}_g\sigma_g^2 + \mathbf{A}_t\sigma_t^2 + \mathbf{A}_m\sigma_m^2 + \mathbf{I}\sigma_e^2$
461 where $\mathbf{W}_g$, $\mathbf{W}_t$, and $\mathbf{W}_m$ are the matrices of standardised SNP genotypes, gene expression measures,
462 and DNAm levels, respectively, with the corresponding effects $\mathbf{u}_g$, $\mathbf{u}_t$ and $\mathbf{u}_m$; $\mathbf{A}_g = \mathbf{W}_g\mathbf{W}_g'/m_g$ is the
463 genomic relationship matrix (GRM) with m_g being the number of SNPs, $\mathbf{A}_t = \mathbf{W}_t\mathbf{W}_t'/m_t$ is the
464 transcriptomic relationship matrix (TRM) with m_t being the number of transcripts, and $\mathbf{A}_m =$
465 $\mathbf{W}_m\mathbf{W}_m'/m_m$ is the methylomic relationship matrix (MRM) with m_m being the number of DNAm
466 probes. Note that the model can be reduced by dropping any of the variance components or
467 expanded by including other types of omic profiles (e.g., protein abundance).
468
469 **Dataset**
470 The LBC cohorts [52, 53] consisted of individuals born in 1921 (LBC1921) and 1936 (LBC1936),
471 mostly living in Edinburgh city and the surrounding Lothian region of Scotland. Blood samples were
472 collected with informed consent. The use of human participants in this study was approved by
473 University of Queensland Human Research Ethics Committee B (approval number: 2011001173).
474 The LBC individuals underwent several waves of SNP genotyping and DNAm measures. DNA
475 methylation levels at 485,512 CpG sites across the genome were measured on 3,191 whole blood
476 samples from 3 waves using the Illumina HumanMethylation450 BeadChip. Duplicates or samples
477 with an excessive proportion of low confidence calls across all probes (>5%) were removed. Probes
478 with an excessive proportion of low confidence calls across all individuals (>5%) or probes located
479 in sex chromosomes were excluded. In addition, probes encompassing SNPs annotated in dbSNP131
480 using hg19 coordinates or identified as potentially cross-hybridized methylation probes by a
481 previous study [54] were also excluded. After these QC steps, 3,018 samples and 307,360 probes
482 remained (**Supplementary Note 3**). We included in the analysis only the first wave (wave1) of the
483 LBC data consisting of 436 individuals from LBC1921 (average age of 79 years) and 906 individuals
484 from LBC1936 (average age of 70 years) (**Supplementary Table 9**). We finally removed probes
485 with almost invariable beta values across individuals (standard deviation < 0.02) and retained 1,342
486 individuals and 228,694 probes for further analysis.
487
488 There were a number of covariates available in the LBC data including age, sex, batches of the
489 experiment (i.e. plate and position of the sample on a chip), and CTCs. The blood cell counts for
490 different cell types, including basophils, eosinophils, monocytes, lymphocytes, and neutrophils,

491 were quantified using an LH50 Beckman Coulter instrument on the same day of blood collection. In
492 addition to the covariates, there are a number of traits measured on the LBC individuals including
493 height (measured without shoes), body mass index (BMI), lung function (measured in the highest
494 score of forced expiratory volume in one second), and walking speed (measured in the time taken to
495 walk 6 metres) and smoking status (never smoked, ex-smoker or current smoker) [55, 56]. The
496 numbers of missing measurements are noted in **Supplementary Table 10**. For each trait, we
497 adjusted the phenotype for age in each gender group of each cohort (LBC1921 or LBC1936) and
498 standardised the residuals by rank-based inverse normal transformation. This process removes the
499 age effect and potential difference in mean and variance between two gender groups or cohorts.
500
501 The LBC wave1 individuals were also genotyped by Illumina 610-Quadv1 BeadChip. The QC process
502 of the SNP genotype data has been detailed elsewhere [14]. After excluding SNPs from sex
503 chromosomes and SNPs with low allelic frequency (MAF < 0.01), we retained 523,062 genotyped
504 SNPs for analysis.
505
506 **URLs**
507 OSCA, http://cnsgenomics.com/software/osca;
508 ReFACTor, https://www.cs.tau.ac.il/~heran/cozygene/software/refactor.html;
509 EWASher, https://www.microsoft.com/en-us/research/project/fast-lmm-software-papers/;
510 SVA, https://bioconductor.org/packages/release/bioc/html/sva.html;
511 LFMM2, https://bcm-uga.github.io/lfmm/;
512
513 **Data availability**
514 The LBC data are available at https://www.ebi.ac.uk/ega/studies/EGAS00001000910.
515
516 **Acknowledgements**
517 This research was supported by the Australian National Health and Medical Research Council
518 (grants 1107258, 1113400, 1083656, 1078037, and 1078901) and the Sylvia & Charles Viertel
519 Charitable Foundation. The Lothian Birth Cohorts (LBC) are supported by Age UK (Disconnected
520 Mind programme). Methylation typing was supported by Centre for Cognitive Ageing and Cognitive
521 Epidemiology (Pilot Fund award), Age UK, The Wellcome Trust Institutional Strategic Support Fund,
522 The University of Edinburgh, and The University of Queensland. The LBC resource is prepared in the
523 Centre for Cognitive Ageing and Cognitive Epidemiology, which is supported by the Medical

Research Council and Biotechnology and Biological Sciences Research Council (MR/K026992/1), and which supports I.J.D..

Author contributions

J.Y. conceived the study. J.Y. and F.Z. designed the experiment. F.Z. developed the software tool and performed all the analyses under the guidance and/or assistance from J.Y., Z.Z., W.C. and Q.Z.. J.Y., A.F.M., P.M.V. and N.R.W. contributed funding and resources. I.J.D., P.M.V. and N.R.W. contributed the DNA methylation data. F.Z., J.Y. and W.C. wrote the manuscript with the participation of all authors.

References

1. Ritchie MD, Holzinger ER, Li R, Pendergrass SA, Kim D: **Methods of integrating data to uncover genotype-phenotype interactions.** *Nat Rev Genet* 2015, **16:**85-97.
2. Hasin Y, Seldin M, Lusis A: **Multi-omics approaches to disease.** *Genome Biol* 2017, **18:**83.
3. Wu Y, Zeng J, Zhang F, Zhu Z, Qi T, Zheng Z, Lloyd-Jones LR, Marioni RE, Martin NG, Montgomery GW, et al: **Integrative analysis of omics summary data reveals putative mechanisms underlying complex traits.** *Nat Commun* 2018, **9:**918.
4. Consortium GT, Laboratory DA, Coordinating Center -Analysis Working G, Statistical Methods groups-Analysis Working G, Enhancing Gg, Fund NIHC, Nih/Nci, Nih/Nhgri, Nih/Nimh, Nih/Nida, et al: **Genetic effects on gene expression across human tissues.** *Nature* 2017, **550:**204-213.
5. Lloyd-Jones LR, Holloway A, McRae A, Yang J, Small K, Zhao J, Zeng B, Bakshi A, Metspalu A, Dermitzakis M, et al: **The Genetic Architecture of Gene Expression in Peripheral Blood.** *Am J Hum Genet* 2017, **100:**371.
6. Hannon E, Spiers H, Viana J, Pidsley R, Burrage J, Murphy TM, Troakes C, Turecki G, O'Donovan MC, Schalkwyk LC, et al: **Methylation QTLs in the developing brain and their enrichment in schizophrenia risk loci.** *Nat Neurosci* 2016, **19:**48-54.
7. Jaffe AE, Gao Y, Deep-Soboslay A, Tao R, Hyde TM, Weinberger DR, Kleinman JE: **Mapping DNA methylation across development, genotype and schizophrenia in the human frontal cortex.** *Nat Neurosci* 2016, **19:**40-47.
8. Grubert F, Zaugg JB, Kasowski M, Ursu O, Spacek DV, Martin AR, Greenside P, Srivas R, Phanstiel DH, Pekowska A, et al: **Genetic Control of Chromatin States in Humans Involves Local and Distal Chromosomal Interactions.** *Cell* 2015, **162:**1051-1065.
9. Chen L, Ge B, Casale FP, Vasquez L, Kwan T, Garrido-Martin D, Watt S, Yan Y, Kundu K, Ecker S, et al: **Genetic Drivers of Epigenetic and Transcriptional Variation in Human Immune Cells.** *Cell* 2016, **167:**1398-1414 e1324.
10. Battle A, Khan Z, Wang SH, Mitrano A, Ford MJ, Pritchard JK, Gilad Y: **Genomic variation. Impact of regulatory variation from RNA to protein.** *Science* 2015, **347:**664-667.
11. Folkersen L, Fauman E, Sabater-Lleal M, Strawbridge RJ, Franberg M, Sennblad B, Baldassarre D, Veglia F, Humphries SE, Rauramaa R, et al: **Mapping of 79 loci for 83 plasma protein biomarkers in cardiovascular disease.** *PLoS Genet* 2017, **13:**e1006706.
12. Wahl S, Drong A, Lehne B, Loh M, Scott WR, Kunze S, Tsai PC, Ried JS, Zhang W, Yang Y, et al: **Epigenome-wide association study of body mass index, and the adverse outcomes of adiposity.** *Nature* 2017, **541:**81-86.
13. Gusev A, Mancuso N, Won H, Kousi M, Finucane HK, Reshef Y, Song L, Safi A, Schizophrenia Working Group of the Psychiatric Genomics C, McCarroll S, et al: **Transcriptome-wide**

association study of schizophrenia and chromatin activity yields mechanistic disease insights. *Nat Genet* 2018, **50:**538-548.

14. Shah S, Bonder MJ, Marioni RE, Zhu Z, McRae AF, Zhernakova A, Harris SE, Liewald D, Henders AK, Mendelson MM, et al: **Improving Phenotypic Prediction by Combining Genetic and Epigenetic Associations.** *Am J Hum Genet* 2015, **97:**75-85.
15. van Kessel KEM, van der Keur KA, Dyrskjot L, Algaba F, Welvaart NYC, Beukers W, Segersten U, Keck B, Maurer T, Simic T, et al: **Molecular Markers Increase Precision of the European Association of Urology Non-Muscle-Invasive Bladder Cancer Progression Risk Groups.** *Clinical Cancer Research* 2018, **24:**1586-1593.
16. Gamazon ER, Wheeler HE, Shah KP, Mozaffari SV, Aquino-Michaels K, Carroll RJ, Eyler AE, Denny JC, Consortium GT, Nicolae DL, et al: **A gene-based association method for mapping traits using reference transcriptome data.** *Nat Genet* 2015, **47:**1091-1098.
17. Gusev A, Ko A, Shi H, Bhatia G, Chung W, Penninx BW, Jansen R, de Geus EJ, Boomsma DI, Wright FA, et al: **Integrative approaches for large-scale transcriptome-wide association studies.** *Nat Genet* 2016, **48:**245-252.
18. Zhu Z, Zhang F, Hu H, Bakshi A, Robinson MR, Powell JE, Montgomery GW, Goddard ME, Wray NR, Visscher PM, Yang J: **Integration of summary data from GWAS and eQTL studies predicts complex trait gene targets.** *Nat Genet* 2016, **48:**481-487.
19. Liu Y, Aryee MJ, Padyukov L, Fallin MD, Hesselberg E, Runarsson A, Reinius L, Acevedo N, Taub M, Ronninger M, et al: **Epigenome-wide association data implicate DNA methylation as an intermediary of genetic risk in rheumatoid arthritis.** *Nat Biotechnol* 2013, **31:**142-147.
20. Michels KB, Binder AM, Dedeurwaerder S, Epstein CB, Greally JM, Gut I, Houseman EA, Izzi B, Kelsey KT, Meissner A, et al: **Recommendations for the design and analysis of epigenome-wide association studies.** *Nat Methods* 2013, **10:**949-955.
21. Jaffe AE, Irizarry RA: **Accounting for cellular heterogeneity is critical in epigenome-wide association studies.** *Genome Biology* 2014, **15**.
22. Leek JT, Storey JD: **Capturing heterogeneity in gene expression studies by surrogate variable analysis.** *PLoS Genet* 2007, **3:**1724-1735.
23. Teschendorff AE, Zheng SC: **Cell-type deconvolution in epigenome-wide association studies: a review and recommendations.** *Epigenomics* 2017, **9:**757-768.
24. Teschendorff AE, Relton CL: **Statistical and integrative system-level analysis of DNA methylation data.** *Nat Rev Genet* 2018, **19:**129-147.
25. Rakyan VK, Beyan H, Down TA, Hawa MI, Maslau S, Aden D, Daunay A, Busato F, Mein CA, Manfras B, et al: **Identification of type 1 diabetes-associated DNA methylation variable positions that precede disease diagnosis.** *PLoS Genet* 2011, **7:**e1002300.
26. Teschendorff AE, Menon U, Gentry-Maharaj A, Ramus SJ, Gayther SA, Apostolidou S, Jones A, Lechner M, Beck S, Jacobs IJ, Widschwendter M: **An epigenetic signature in peripheral blood predicts active ovarian cancer.** *PLoS One* 2009, **4:**e8274.
27. Guintivano J, Aryee MJ, Kaminsky ZA: **A cell epigenotype specific model for the correction of brain cellular heterogeneity bias and its application to age, brain region and major depression.** *Epigenetics* 2013, **8:**290-302.
28. Houseman EA, Accomando WP, Koestler DC, Christensen BC, Marsit CJ, Nelson HH, Wiencke JK, Kelsey KT: **DNA methylation arrays as surrogate measures of cell mixture distribution.** *Bmc Bioinformatics* 2012, **13**.
29. Gagnon-Bartsch JA, Speed TP: **Using control genes to correct for unwanted variation in microarray data.** *Biostatistics* 2012, **13:**539-552.
30. Zou J, Lippert C, Heckerman D, Aryee M, Listgarten J: **Epigenome-wide association studies without the need for cell-type composition.** *Nat Methods* 2014, **11:**309-311.

617 31. Rahmani E, Zaitlen N, Baran Y, Eng C, Hu D, Galanter J, Oh S, Burchard EG, Eskin E, Zou J,
618 Halperin E: **Sparse PCA corrects for cell type heterogeneity in epigenome-wide**
619 **association studies.** *Nat Methods* 2016, **13:**443-445.
620 32. Caye K, Jumentier B, Francois O: **LFMM 2.0: Latent factor models for confounder**
621 **adjustment in genome and epigenome-wide association studies.** *bioRxiv* 2018.
622 33. Patterson HD, Thompson R: **Recovery of Inter-Block Information When Block Sizes Are**
623 **Unequal.** *Biometrika* 1971, **58:**545-+.
624 34. Yang J, Benyamin B, McEvoy BP, Gordon S, Henders AK, Nyholt DR, Madden PA, Heath AC,
625 Martin NG, Montgomery GW, et al: **Common SNPs explain a large proportion of the**
626 **heritability for human height.** *Nat Genet* 2010, **42:**565-569.
627 35. Yang J, Lee SH, Goddard ME, Visscher PM: **GCTA: a tool for genome-wide complex trait**
628 **analysis.** *Am J Hum Genet* 2011, **88:**76-82.
629 36. Henderson CR: **Best linear unbiased estimation and prediction under a selection model.**
630 *Biometrics* 1975, **31:**423-447.
631 37. Zhou X, Stephens M: **Genome-wide efficient mixed-model analysis for association studies.**
632 *Nat Genet* 2012, **44:**821-824.
633 38. Kang HM, Sul JH, Service SK, Zaitlen NA, Kong SY, Freimer NB, Sabatti C, Eskin E: **Variance**
634 **component model to account for sample structure in genome-wide association studies.**
635 *Nat Genet* 2010, **42:**348-354.
636 39. Yang J, Zaitlen NA, Goddard ME, Visscher PM, Price AL: **Advantages and pitfalls in the**
637 **application of mixed-model association methods.** *Nat Genet* 2014, **46:**100-106.
638 40. Lippert C, Listgarten J, Liu Y, Kadie CM, Davidson RI, Heckerman D: **FaST linear mixed models**
639 **for genome-wide association studies.** *Nat Methods* 2011, **8:**833-835.
640 41. Meissner A, Mikkelsen TS, Gu H, Wernig M, Hanna J, Sivachenko A, Zhang X, Bernstein BE,
641 Nusbaum C, Jaffe DB, et al: **Genome-scale DNA methylation maps of pluripotent and**
642 **differentiated cells.** *Nature* 2008, **454:**766-770.
643 42. Laurent L, Wong E, Li G, Huynh T, Tsirigos A, Ong CT, Low HM, Kin Sung KW, Rigoutsos I, Loring
644 J, Wei CL: **Dynamic changes in the human methylome during differentiation.** *Genome Res*
645 2010, **20:**320-331.
646 43. McGregor K, Bernatsky S, Colmegna I, Hudson M, Pastinen T, Labbe A, Greenwood CM: **An**
647 **evaluation of methods correcting for cell-type heterogeneity in DNA methylation studies.**
648 *Genome Biol* 2016, **17:**84.
649 44. Starr JM, Deary IJ: **Sex differences in blood cell counts in the Lothian Birth Cohort 1921**
650 **between 79 and 87 years.** *Maturitas* 2011, **69:**373-376.
651 45. Devlin B, Roeder K: **Genomic control for association studies.** *Biometrics* 1999, **55:**997-1004.
652 46. Mendelson MM, Marioni RE, Joehanes R, Liu C, Hedman AK, Aslibekyan S, Demerath EW, Guan
653 W, Zhi D, Yao C, et al: **Association of Body Mass Index with DNA Methylation and Gene**
654 **Expression in Blood Cells and Relations to Cardiometabolic Disease: A Mendelian**
655 **Randomization Approach.** *PLoS Med* 2017, **14:**e1002215.
656 47. Gao X, Jia M, Zhang Y, Breitling LP, Brenner H: **DNA methylation changes of whole blood cells**
657 **in response to active smoking exposure in adults: a systematic review of DNA**
658 **methylation studies.** *Clin Epigenetics* 2015, **7:**113.
659 48. Shenker NS, Polidoro S, van Veldhoven K, Sacerdote C, Ricceri F, Birrell MA, Belvisi MG, Brown
660 R, Vineis P, Flanagan JM: **Epigenome-wide association study in the European Prospective**
661 **Investigation into Cancer and Nutrition (EPIC-Turin) identifies novel genetic loci**
662 **associated with smoking.** *Hum Mol Genet* 2013, **22:**843-851.
663 49. Listgarten J, Lippert C, Kadie CM, Davidson RI, Eskin E, Heckerman D: **Improved linear mixed**
664 **models for genome-wide association studies.** *Nat Methods* 2012, **9:**525-526.

50. Peters MJ, Joehanes R, Pilling LC, Schurmann C, Conneely KN, Powell J, Reinmaa E, Sutphin GL, Zhernakova A, Schramm K, et al: **The transcriptional landscape of age in human peripheral blood.** *Nat Commun* 2015, **6:**8570.
51. Zhang Q, Vallerga C, Walker R, Lin T, Henders A, Montgomery G, He J, Fan D, Fowdar J, Kennedy M, et al: **Improved prediction of chronological age from DNA methylation limits it as a biomarker of ageing.** *bioRxiv* 2018.
52. Deary IJ, Gow AJ, Pattie A, Starr JM: **Cohort profile: the Lothian Birth Cohorts of 1921 and 1936.** *Int J Epidemiol* 2012, **41:**1576-1584.
53. Taylor AM, Pattie A, Deary IJ: **Cohort Profile Update: The Lothian Birth Cohorts of 1921 and 1936.** *Int J Epidemiol* 2018, **47:**1042-1042r.
54. Price ME, Cotton AM, Lam LL, Farre P, Emberly E, Brown CJ, Robinson WP, Kobor MS: **Additional annotation enhances potential for biologically-relevant analysis of the Illumina Infinium HumanMethylation450 BeadChip array.** *Epigenetics Chromatin* 2013, **6:**4.
55. Deary IJ, Whiteman MC, Starr JM, Whalley LJ, Fox HC: **The impact of childhood intelligence on later life: following up the Scottish mental surveys of 1932 and 1947.** *J Pers Soc Psychol* 2004, **86:**130-147.
56. Deary IJ, Gow AJ, Taylor MD, Corley J, Brett C, Wilson V, Campbell H, Whalley LJ, Visscher PM, Porteous DJ, Starr JM: **The Lothian Birth Cohort 1936: a study to examine influences on cognitive ageing from age 11 to age 70 and beyond.** *BMC Geriatr* 2007, **7:**28.

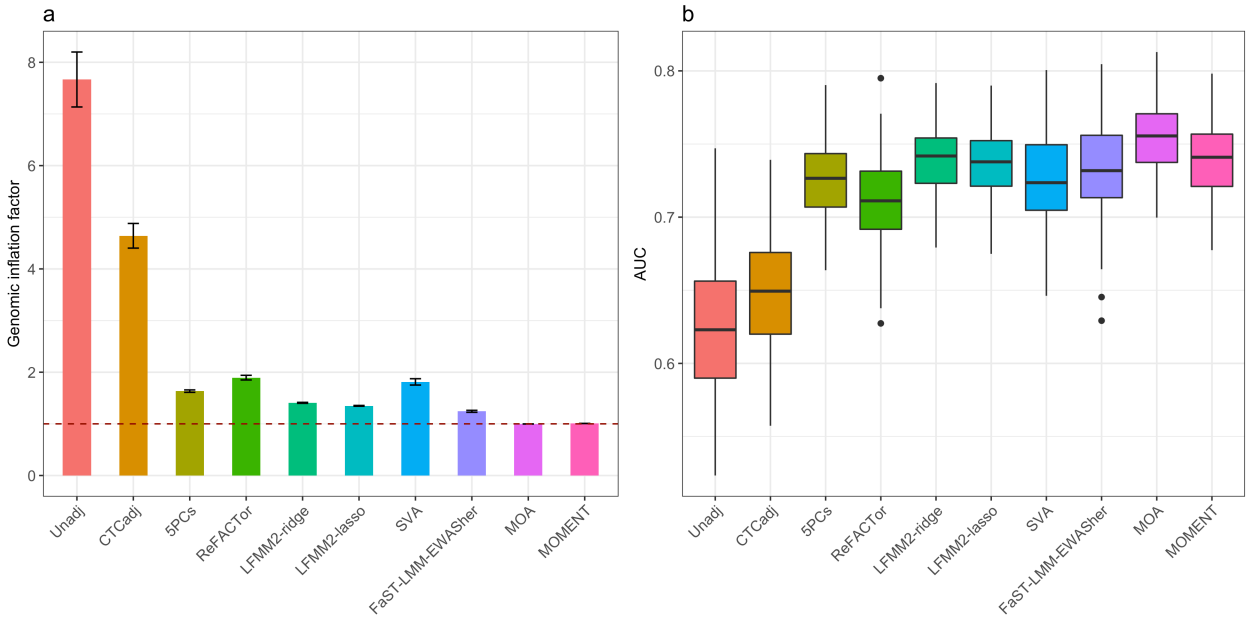

Figure 1 Power and false positive rate for the MWAS methods in simulation scenario 1. The phenotypes were simulated based on the effects from 100 causal probes but no direct effects from the CTCs. (a) Mean genomic inflation factor from a method across 100 simulation replicates with an error bar representing +/- SE of the mean. The dashed line at 1 shows the expected value if there is no inflation. (b) Box plot of AUCs for each method from 100 simulation replicates.

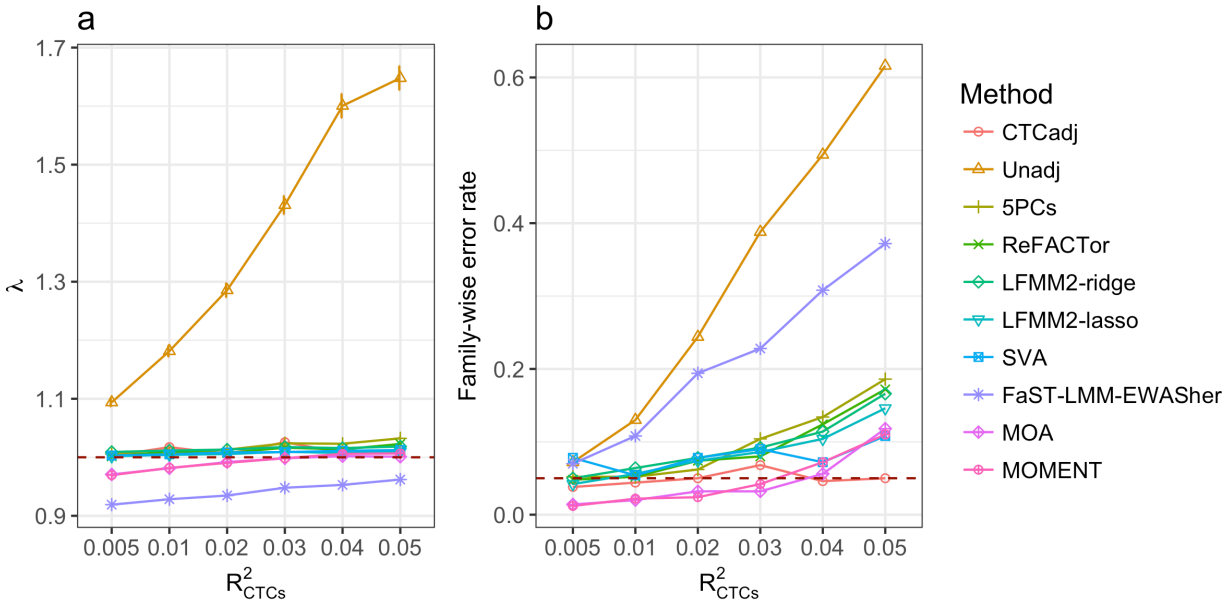

Figure 2 Genomic inflation factor and family-wise error rate for the MWAS methods in simulation scenario 2 (effects from CTCs but no causal probes). Shown on the horizontal axis are the R^2_{CTCs} values used to simulate the phenotype. (a) Each dot represents the mean λ value from 1000 simulation replicates given a specified R^2_{CTCs} value for a method with an error bar representing +/- the SE of the mean. (b) Each dot represents the family-wise error rate, calculated as the proportion of simulation replicates with one or more null probes detected at a genome-wide significance level.

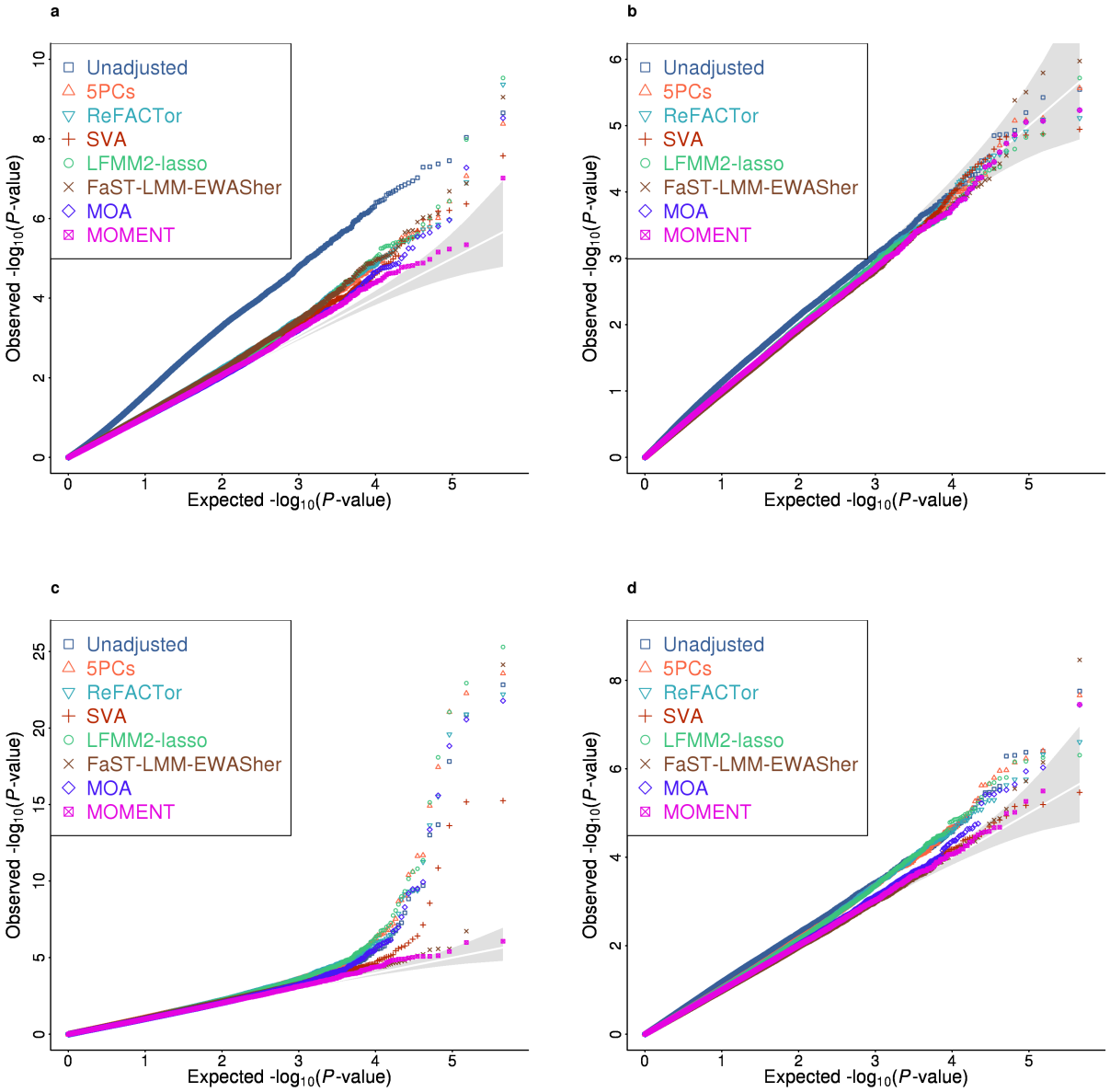

Figure 3 QQ plot of p-values from MWAS analysis for 4 quantitative traits in the LBC data. The DNAm measures were adjusted for age, sex, and batches. The phenotypes were stratified into groups by sex and cohort and were adjusted for age and standardised to z-scores by rank-based inverse normal transformation in each group. The phenotypes are (a) BMI, (b) height (c) lung function, and (d) walking speed.

705 **Table 1** Genomic inflation factors reported by different MWAS methods for the 4 traits in the
706 Lothian Birth Cohorts.

	BMI	Height	Lung function	Walking speed
Unadjusted	1.68	1.30	0.98	1.28
5PCs	1.11	0.96	1.06	1.04
SVA	1.04	0.95	1.06	1.01
LFMM2-ridge	1.09	1.00	1.10	1.04
LFMM2-lasso	1.08	0.99	1.09	1.03
ReFACTor	1.13	0.97	1.09	1.02
EWASher	1.11	0.96	1.09	0.96
MOA	0.99	1.02	0.97	0.99
MOMENT	1.00	1.02	0.98	1.00

707